P9.86 RETRIEVAL OF MICROPHYSICAL PROPERTIES FOR THE MIXTURE OF RAIN AND HAIL USING DOPPLER SPECTRAL ANALYSIS AND GENETIC ALGORITHM

Yadong Wang[1] * and Tian-You Yu[2,3], Xiao Xiao[2,3]

[1] Cooperative Institute for Mesoscale Meteorological Studies, University of Oklahoma, Norman, OK, USA
[2] School of Electrical and Computer Engineering, University of Oklahoma, Norman, Oklahoma, USA
[3] Atmospheric Radar Research Center, University of Oklahoma, Norman, Oklahoma, USA

1. INTRODUCTION

The mixed-phase precipitation that comprises either rain and hail or graupel and hail are commonly observed below or above the melting level, respectively [Pruppacher and Pitter, 1971]. This mixture can be frequently observed in convective storms, where water can exist at temperatures below 0^{o}C and ice can be found at temperature above 0^{o}C [Balakrishnan and Zrnić, 1990]. For melting hailstones, their scattering properties become close to pure ice (if the percentage of ice is very high) or pure water (if the percentage of water is high). It was demonstrated that even for the same mixture of rain and hail (same rainrate and hail rate), after the hailstones start to melt, the reflectivity Z, the differential reflectivity Z_{DR} and the differential propagation constant K_{DP} show different values with different water percentages in the hailstones [Balakrishnan and Zrnić, 1990]. Overestimation of hailrate will be generated if the melting is not considered. Therefore, it is valuable to accurately estimate the water fraction of the melting hailstones.

The DSD is one of the most important parameters to be determined in weather radar, since the relation between the received power from precipitation and the rainfall and/or the hailrate are largely affected by the size of drops. The DSDs of both raindrops and melting hailstones and the melting ratio are proposed to be retrieved simultaneously based on the measurements of Doppler spectra and Z_{DR} spectra. In this work, the model of Doppler and polarimetric spectra and the retrieval algorithm are developed for C-band radars. This work is organized as follows. An overview of the microphysical properties of raindrops and hailstones is presented in section 2. The retrieval of DSD and melting ratio using dual-polarization spectra is developed in section 3. The sensitivity analysis and the retrieval procedure are presented in section 4 and section 5. The retrieval algorithm is evaluated in section 6. Finally, the conclusions and future work are given in section 7

* *Corresponding author address:* Yadong Wang, Yadong Wang, Cooperative Institute for Mesoscale Meteorological Studies, University of Oklahoma, Norman, Oklahoma 73072; e-mail: Yadong.wang@noaa.gov

2. MICROPHYSICAL PROPERTIES OF RAINDROP AND HAILSTONE

2.1. *The size, shape, orientation and terminal velocity*

It was shown from observations that smaller raindrops ($<$ 1 mm in diameter) are typically spherical, but larger raindrops ($>$ 1 mm in diameter) normally exhibit the shape of oblate spheroids [Green, 1975]. The axis ratio (r), representing the ratio between minor to major axis, is related to the equivalent diameters (D) in an equilibrium model [Green, 1975]. The polynomial function developed by Zhang et al. [2001] is used in this work to describe the raindrop's relationship. The hailstone size has been reported to be as large as 50 mm in diameter [Battan and Theiss, 1973]. However, most of the hailstones have been observed within the range of 5 - 25 mm [e.g., Matson and Huggins, 1980; Mitchell, 1996], which is the hailstone size used in this study. The majority of hailstones have been reported with an axis ratio of between 0.6 and 0.8 based on the ground observations [Matson and Huggins, 1980; Knight, 1982], and the value of 0.75 was used in Jung et al. [2007]. In this work, the axis ratio of hailstones is set to be 0.75 and the axis ratio for raindrops is estimated using [Zhang et al., 2001; Jung et al., 2007]. Furthermore, it is assumed that the major axis of a falling particles is aligned in the horizontal direction [Jung et al., 2007].

The terminal velocity of raindrop and hailstones used in this work is followed the work from [Atlas et al., 1973] and Mitchell [1996], respectively. The radial velocity observed by a weather radar with elevation angle of γ can be written as follows.

$$v(D) = V_t(D) \times \sin(\gamma) + v_0 \quad (1)$$

where v_t is particle's terminal velocity and v_0 is the ambient air radial velocity (m s^{-1}).

2.2. The drop size distribution (DSD)

Based on earlier observations [e.g., Marshall and Palmer, 1948; Law and Parson, 1943], the exponential DSD was derived in the following equation.

$$N(D) = N_w \exp(-\Lambda D) \tag{2}$$

Ulbrich [1983] suggested the use of the Gamma distribution for representing raindrop DSD.

$$N(D) = N_w D^{\mu} \exp(-\Lambda D) \tag{3}$$

The Gamma DSD with three parameters (N_w, μ and Λ) is capable of describing a broader variation in rain DSD than an exponential distribution. It should be noted that the exponential distribution is a special case of Gamma distribution with μ = 0. More accurate and complicated expression of Gamma distribution was suggested by Bringi and Chandrasekar [2001] as:

$$\begin{aligned} N(D) \quad = \quad & N_w \frac{6}{3.67^4} \frac{(3.67+\mu)^{\mu+4}}{\Gamma(\mu+4)} (\frac{D}{D_0})^{\mu} \\ & \exp[-(3.67+\mu)\frac{D}{D_0}] \end{aligned} \tag{4}$$

where N_w, D_0 and μ are the intercept parameter of the distribution, median volume diameter of a raindrop, and the shape parameter, respectively. Note that for hailstones, the exponential DSD of Eq. (2) is often used [e.g., Cheng and English, 1983; Balakrishnan and Zrnić, 1990; Spek et al., 2007], where Λ and D are in mm^{-1} and mm, respectively.

2.3. Melting process of hailstone

The melting process of ice particles is closely related to the latent heat transfer and the redistribution of liquid water in cloud, and have been studies in plentiful work [e.g., Rasmussen et al., 1984a,b; Rasmussen and Heymsfield, 1987]. It was reported that smaller size hailstone can carry more water on surface to reach its equilibrium mass, but for larger size hailstone, this water fraction becomes smaller [Rasmussen et al., 1984b; Rasmussen and Heymsfield, 1987]. If the water on the surface of a melting hailstone excesses the the equilibrium mass, shedding will occur. As a result, the mass of water-coated hailstone decreases and consequently the terminal velocity will decrease. In this work, the shedding process is not considered for the simplification purpose. In other words, if the water on the surface of a hailstone reaches its equilibrium mass, the melting process stops and the melting ratio reaches its maximum value. The melting ratio (f_w) of hailstones is defined by Rasmussen et al. [1984b]; Jung et al. [2007] as presented in the following equation.

$$f_w = \frac{m_w}{m_w + m_i} \tag{5}$$

where the m_w is the mass of the melted water on the surface of the hailstones, and m_i are the mass of the ice core. Moreover, no shedding occurs if the equivalent diameter of the melting hailstone is less than 9 mm, which means the f_w of small size hailstone (<9 mm) can be up to 100$\%$ [Rasmussen et al., 1984b]. The water mass growth rate for small (5 mm $< D <$ 9 mm) and large (9 mm $< D <$ 25 mm) hailstones suggested by Rasmussen et al. [1984b].

The melting ratio for different sizes of hailstones can be derived if the melting ratio of the smallest size is known. It is assumed that all the hailstones start to melt at the same moment and the mass of hailstones is conserved during the melting process (i.e., no shedding, collision and condensation are considered). The mass of the hailstone with the smallest diameter of 5 mm is denoted by m_t^{5mm} at initial time. Assuming after t seconds, the water mass on the melting hail is m_w^{5mm}. The melting ratio of the smallest hail at time t can be calculated using the following equation.

$$f_w^{5\mathrm{mm}} = \frac{m_w^{5\mathrm{mm}}}{m_t^{5\mathrm{mm}}} \tag{6}$$

The water mass growth rate can be approximated by the following equation if the period t is not too large.

$$R_m^{5\mathrm{mm}} = m_w^{5\mathrm{mm}}/t. \tag{7}$$

where $R_m^{5\mathrm{mm}}$ is the estimated water mass growth rate. Based on the analysis of Rasmussen et al. [1984b], the water mass growth rate is a function of the hailstone's size (mass), therefore the water growth rate and the water mass for other sizes of hailstones can be calculated as $m_w = R_m t$. Furthermore, the melting ratio of other sizes hailstones can be estimated using Eq. (7).

Given the melting ratio of the smallest hailstone with diameter of 5 mm ($f_w^{5\mathrm{mm}}$), the distribution of melting ratio as a function of the hailstones size is presented in Fig. 1. For small particles (with size less than 9 mm), the melting ratio can be as high as 100$\%$. In other words, it can melt into raindrop. However, for large drop with diameter of 20 mm for example, the maximum melting ratio is below 20$\%$. This result is consistent with the early observations by Rasmussen et al. [1984b]. Note hereafter the melting ratio is used to represent the melting ratio of the smallest hailstone ($F_w = f_w^{5\mathrm{mm}}$), if not specified.

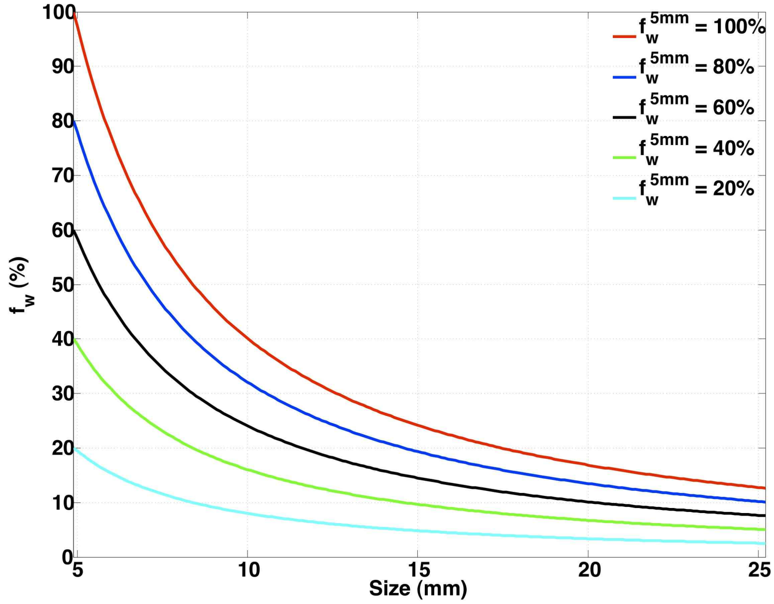

Figure 1: The melting ratio of hailstone as function of hailstones' size. The melting ratio of the smallest hailstone with diameter of 5 mm f_w^{mm} is given and the melting ratio of other size can be estimated. The X axis is the equivalent diameter of hailstone, and Y axis is melting ratio (f_w). Different color lines indicate different melting ratios of the smallest hail.

2.4. Canting angle of raindrop and hailstone

The canting of hydrometeor can be caused by different sources such as ambient wind and turbulence [Spek et al., 2007]. The backscattering cross section can be estimated using the following equations [Zhang et al., 2001; Jung et al., 2007]:

$$\begin{aligned} \sigma_{hh} &= 4\pi < |F_{hh}|^2 > \\ &= 4\pi(\bar{A^2}|f_a|^2 + \bar{B^2}|f_b|^2 + 2\bar{AB}|f_a||f_b|) \end{aligned} \tag{8}$$

$$\begin{aligned} \sigma_{vv} &= 4\pi < |F_{vv}|^2 > \\ &= 4\pi(\bar{D^2}|f_a|^2 + \bar{C^2}|f_b|^2 + 2\bar{CD}|f_a||f_b|) \end{aligned} \tag{9}$$

where the f_a and f_b are the scattering amplitude at horizontal and vertical direction of raindrop and hailstone. In this work, the f_a and f_b are calculated using the T-matrix method following Zhang et al. [2001]. And the $\bar{\phi}$ and σ are the mean and standard deviation (SD) of the canting angles. In this work the mean and standard deviation of the canting angle for raindrop are 0^o, which was suggested based on observations [Hendry and McCormick, 1976], and further implemented by Jung et al. [2007]. For hailstones, the mean of canting angle is also assumed to be 0^o, but the SD is a function of the melting ratio as $\sigma = 60^o(1 - cf_w)$, where c is a coefficient of 0.8 [Jung et al., 2007].

3. RETRIEVAL OF DROP SIZE DISTRIBUTION AND MELTING RATIO USING DUAL-POLARIMETRIC SPECTRA

Assume that there is no spectral broadening, the Doppler spectrum, $S_{hh}(v)dv$ for the horizontal polarization and $S_{vv}(v)dv$ for the vertical polarization and the differential reflectivity spectrum $Z_{DR}(v)dv$ can be written as [Doviak and Zrnić, 1993; Moisseev et al., 2006; Spek et al., 2007]:

$$S_{hh}(v)dv = \frac{\lambda^4}{\pi^5|k_w|^2}N[D(v)]\sigma_{hh}[D(v)]\frac{dD(v)}{dv}dv \tag{10}$$

$$S_{vv}(v)dv = \frac{\lambda^4}{\pi^5|k_w|^2}N[D(v)]\sigma_{vv}[D(v)]\frac{dD(v)}{dv}dv \tag{11}$$

$$Z_{DR}(v)dv = \frac{S_{hh}(v)}{S_{vv}(v)}dv \tag{12}$$

where the dielectric factor $k_w = (\epsilon_r - 1)/(\epsilon_r + 2)$, ϵ_r is the complex dielectric constant calculated using the Maxwell-Garnett mixing formula [Maxwell-Garnett, 1904], $N[D(v)]$ is the DSD (# m^{-3}mm^{-1}). It is apparent that the Doppler spectrum and differential reflectivity spectrum are determined by $N(D)$ and the backscattering cross section of σ_{hh} and σ_{vv}, where D can be determined from the radial component of the terminal velocity if the elevation angle is sufficiently high. Moreover, the σ_{hh} and σ_{vv} can be calculated using the backscattering amplitude f_a and f_b.

If the hailstones start to melt, the hailstones become water coated. Since the relative dielectric constant of water is much higher than ice, $68.2317 + j35.4776$ for water compared to $3.1683 + j0.0006$ for ice at 0^{o}C for 5 GHz for example, the water on the surface of hailstone will significantly affect the backscattering amplitude and consequently, the Doppler and differential reflectivity spectra. Moreover, a water-coated hailstone can produce different backscattering amplitudes for different melting ratio. Therefore, the melted hailstone's backscattering amplitude connects the melting ratio and spectra together, and makes the retrieval of melting ratio using Doppler and Z_{DR} spectrum possible.

In this work, the backscattering amplitude of melted hailstones (f_a and f_b) with diameter from 5 mm to 25 mm (with step of 0.7 mm) and with f_w from 0% to 100% (with setp of 5%) are pre-calculatied at C-band using the T-matrix method [Zhang et al., 2001; Jung et al., 2007]. The real and image parts of backscattering amplitude from smallest (5 mm) and largest (25 mm) hailstone as a function of melting ratio f_w are exemplified in Fig. 2. The one to one relationship between the f_w and the $f_a(f_b)$ is needed, so that in the retrieval the Doppler and Z_{DR} spectra can be directly expressed as the function of f_w in the following forms.

$$S_{hh}(v)dv = \frac{\lambda^4}{\pi^5|k_w|^2}N[D(v)]F_{hh}\{f_w[D(v)]\}\frac{dD(v)}{dv}dv \tag{13}$$

$$S_{vv}(v)dv = \frac{\lambda^4}{\pi^5|k_w|^2}N[D(v)]F_{vv}\{f_w[D(v)]\}\frac{dD(v)}{dv}dv \tag{14}$$

where $\sigma_{hh}[D(v)] = F_{hh}\{f_w[D(v)]\}$ and $\sigma_{vv}[D(v)] = F_{vv}\{f_w[D(v)]\}$, and F_{hh} and F_{vv} are the functions that used to calculate $\sigma_{hh}[D(v)]$ and $\sigma_{vv}[D(v)]$ from $f_w[D(v)]$. In this work, the 3rd, 5th and 7th order polynomial fitting have been tested and the results are presented in Fig. 2 using lines with different colors. For the small particle with equivalent diameter of 5 mm, the fitting results of these three approaches are quite similar. However, for large particle with equivalent diameter of 25 mm (bottom panels), the higher order fitting provides much better results. Although polynomial with order higher than 7$^{\mathrm{th}}$ can provide slight improvement, it requires larger computational power. Therefore, the 7$^{\mathrm{th}}$ polynomial is selected for this work.

The Doppler and Z_{DR} spectra for the mixture of raindrops and melting hailstones can be written as the combination of pure rain and pure melted hail in the following equations.

$$S_{hh}(v)dv = S^r_{hh}(N^r_w, D_0, \mu)dv + S^h_{hh}(N^h_w, \Lambda, f_w)dv \tag{15}$$

$$Z_{DR}(v)dv = \frac{S^r_{hh}(N^r_w, D_0, \mu)dv + S^h_{hh}(N^h_w, \Lambda, f_w)dv}{S^r_{vv}(N^r_w, D_0, \mu)dv + S^h_{vv}(N^h_w, \Lambda, f_w)dv} \tag{16}$$

where superscript r and h represent pure rain and melting hail, respectively. It should be noted that the Doppler and Z_{DR} spectra are obtained from sufficiently high elevation angle. Therefore, the separation in spectral components can be obtained from the particles' terminal velocities.

Several factors could produce spectrum broadening such as turbulence, antenna motion, shear and the change in orientation or vibration of hydrometeors [Doviak and Zrnić, 1993]. It is common to model the effect of spectral broadening as a convolution of the original spectrum from precipitation with a Gaussian kernel [Doviak and Zrnić, 1993]:

$$\begin{aligned} S^{mod}_{hh}(v) &= S_{broad}(v) * S_{hh}(v) \\ &= \frac{1}{\sqrt{2\pi}\sigma_b}\int \exp[-\frac{(v-\bar{v})^2}{2\sigma_b^2}]S_{hh}(\bar{v})d\bar{v} \end{aligned} \tag{17}$$

where $S^{mod}_{hh}(v)$ is the model spectrum used in the retrieval procedure, the asterisk (*) is the convolution operator, and σ_b is the width of the Gaussian Kernel (m s^{-1}). This broadening could be the summation of independent contributions, that is $\sigma_b^2 = \sigma_s^2 + \sigma_\alpha^2 + \sigma_o^2 + \sigma_t^2$.

4. SENSITIVITY ANALYSIS

Before the discussion of the retrieval technique, it is necessary to verify that the DSD parameters from both raindrops and hailstones, melting ratio, ambient wind, and spectrum broadening have impacts on the Doppler and differential reflectivity spectra. If the parameter of interest cannot produce noticeable changes, it is not likely to be retrieved correctly and reliably. In this testing, only one parameter is changed while others are kept constant each time. As a result, we can study the dependence of spectrum on the parameter of interest independently. The effect of ambient wind v_0 on the spectrum is straightforward, which can shift the Doppler spectrum by an amount of v_0 according to Eq. (1). In the test, the v_0 is set as 0 and the retrieval of v_0 is discussed in Section 6.1. The simulation is designed for C-band radar, and the ambiguous velocity is set at 16 m s^{-1} in this study. Therefore velocity aliasing can be observed if the radial component of the terminal velocities is larger than

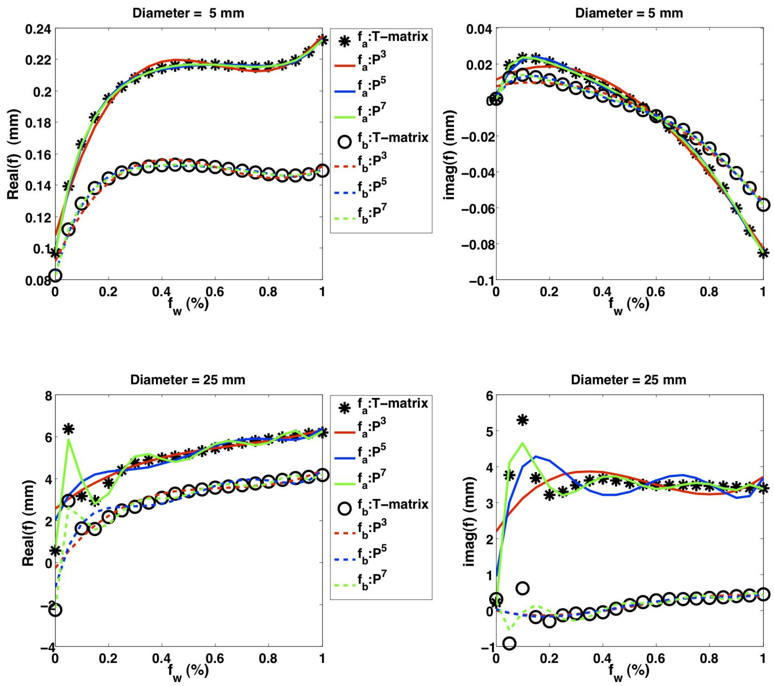

Figure 2: Polarimetric backscattering amplitudes (f_a and f_b as a function of equivolume diameter. The results from T-matrix are denoted by asterisks. The polynomial fitting of the T-matrix results is denoted by red, blue and green lines for the 3rd, 5th and 7th order fittings, respectively.

16 m s^{-1}. It is important and of interest to study the impacts of D_0 and μ from raindrops and f_w, N_w^h and Λ from hailstones on Doppler and Z_{DR} spectra from a mixture of raindrops and melting hailstones. The impact of σ_b on the mixture spectrum is also included in this section.

The conclusions are summarized in the following.

1. D_0 and μ change the low velocity portion (defined by velocity from -8 to 0 m s^{-1}) of the spectrum (from raindrops); and the f_w, N_w^h and Λ only change the high velocity portion (defined by velocity from -16 to -8 m s^{-1}) of the spectrum (from hailstones).

2. The Λ has the most significant impact on Doppler spectrum.

3. Spectrum broadening σ_b smoothen the spectrum from both raindrops and hailstones. The Doppler spectrum with double-peak feature (one from raindrops and the other is from hailstones) can only be observed for smaller σ_b of 0.4 m s^{-1}.

In this section, the dependence of Doppler spectrum and Z_{DR} spectrum on the DSD, melting ratio and spectrum broadening was investigated. It is obvious that D_0, Λ, N_w^h, f_w and σ_b have significant impact on the shape and amplitude of the Doppler spectrum, and D_0, f_w and σ_b have obvious impact on the Z_{DR} spectrum. Those five parameters are likely to be retrieved more accurately. On the other hand, N_w^r and μ have small impact on Doppler spectra, and N_w^r does not affect the Z_{DR} spectrum, therefore can not be retrieved as accurate as previous five parameters.

5. RETRIEVAL OF PARTICLES' DSDS AND THE MELTING RATIO

From previous analysis, it is clear that the model of Doppler spectrum and differential reflectivity spectrum is determined by eight parameters of N_w^r, D_0, μ, N_w^h, Λ, F_w, σ_b and v_0. Therefore, one can formulate the retrieval problem as an optimization of fitting observations to model spectra described in the following.

$$\begin{gathered}\min_{N_w^r, D_0, \mu, N_w^h, \Lambda, F_w, \sigma_b, v_0} \sum_{v=-v_a}^{v_a} \\ \{\log[S_{hh}^{mod}(v, N_w^r, D_0, \mu, N_w^h, \Lambda, F_w, \sigma_b, v_0)dv] \\ -\log[S_{hh}^{meas}(v)dv]\}^2\end{gathered} \tag{18}$$

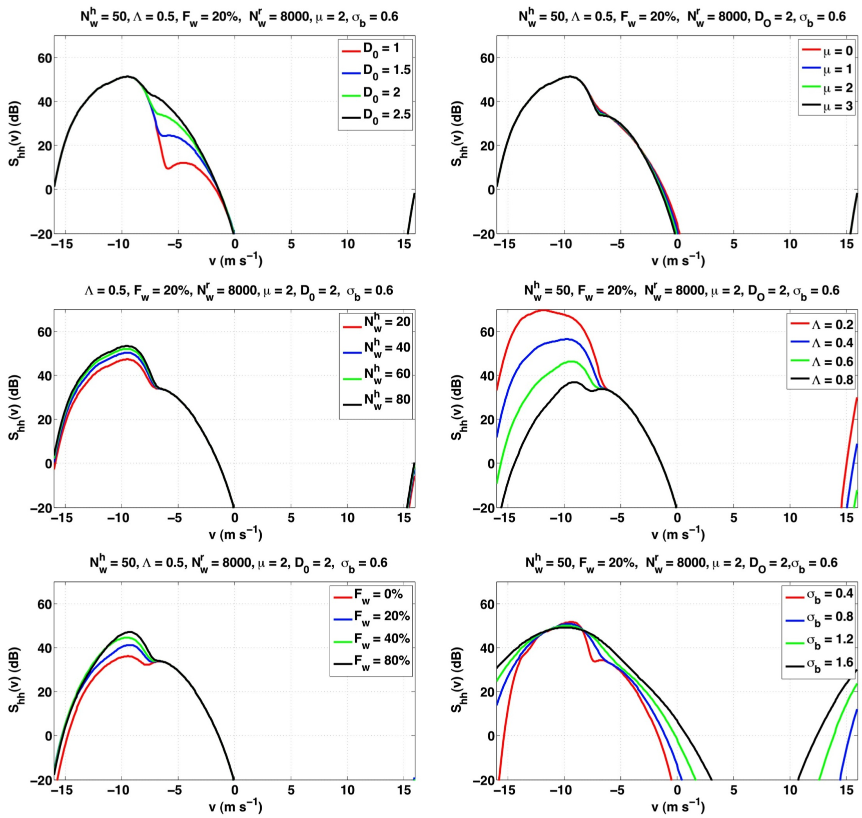

Figure 3: The melting ratio of hailstone as function of hailstones' size. The melting ratio of the smallest hailstone with diameter of 5 mm f_w^{mm} is given and the melting ratio of other size can be estimated. The X axis is the equivalent diameter of hailstone, and Y axis is melting ratio (f_w). Different color lines indicate different melting ratios of the smallest hail.

$$\min_{N_w^r, D_0, \mu, N_w^h, \Lambda, F_w, \sigma_b, v_0} \sum_{v=-v_a}^{v_a} \{\log[Z_{DR}^{mod}(v, N_w^r, D_0, \mu, N_w^h, \Lambda, F_w, \sigma_b, v_0)dv] - \log[Z_{DR}^{meas}(v)dv]\}^2 \tag{19}$$

where S_{hh}^{meas} and Z_{DR}^{meas} are the measured Doppler and differential reflectivity spectra, and S_{hh}^{mod} and Z_{DR}^{mod} are the modeled Doppler spectrum and differential reflectivity spectra defined in Eq. (15) and (16), respectively. In order to suppress the statistical fluctuation, the optimization is performed in the log-domain [Sato et al., 1990]. Similar approach is also adopted in the work of Moisseev et al. [2006] and Spek et al. [2007].

5.1. Introduction of genetic algorithm

The nonlinear least square fitting method, such as Levenberg-Marquardt Algorithm (LMA), is usually implemented in the retrieval process [e.g., Sato et al., 1990; Moisseev et al., 2006; Spek et al., 2007]. In this work, the Genetic Algorithm (GA), which can solve both constrained and unconstrained optimization problems based on natural selection, is proposed for the retrieval. The GA can be used to solve a variety of optimization problems that are not well suited for standard optimization algorithms, including problems in which the objective function is discontinuous, nondifferentiable, stochastic, or highly nonlinear. Compared to traditional deterministic optimization algorithms such as LMA, the GA strategy can increase the probability of obtaining the global minimum instead of local minimum [Sellami et al., 2007]. The GA repeatedly modifies the population of individual solutions. At each step, the GA selects individuals from the current population termed parents and uses them to produce the children for the next generation. Over successive generations, the population "evolves" toward an optimal solution. A model of Doppler and Z_{DR} spectra is first developed using 8 parameters of the DSD of raindrops and melting hailstones (5 parameters), melting ratio, ambient radial velocity, and turbulence broadening. The GA is introduced to estimate the 8 parameters based on the minimization between the model and observed spectra. The GA retrieval for this work is summarized in the following steps.

1. In the retrieval problem, the N_w^r, f_w, ... are the individuals, and the fitness function is defined by the following two equations.

$$f_1(\Upsilon) = \sum_{v=-v_a}^{v_a} \{\log[S_{hh}^{mod}(v, \Upsilon)dv] - \log[S_{hh}^{meas}(v)dv]\}^2 \tag{20}$$

$$f_2(\Upsilon) = \sum_{v=-v_a}^{v_a} \{\log[Z_{DR}^{mod}(v, \Upsilon)dv] - \log[Z_{DR}^{meas}(v)dv]\}^2 \tag{21}$$

where Υ is used to represent the population which is the set of the 8 parameters $(N_w^r, D_0, \mu, N_w^h, \Lambda, F_w, \sigma_b, v_0)$. The algorithm begins by creating a random initial population. If the first guess of each individual can be provided, the initial population will be around the first guess.

2. The value of the fitness function for the current population is computed and scored. A group of individuals associated with better (lower) fitness values in the current population is selected as parents (also called elite), and others are eliminated from current population.

3. Those parents are used to create the children that make up the next generation. Three ways can be used to create children for the next generation: the children from survived elite parent; the crossover children created by combining the vectors of a pair of parents; and the mutation children created by introducing random changes to parents. In this retrieval problem, the method of crossover and mutation children is used.

4. The current generation is replaced by a new generation. Repeat the first three steps until the global optimal fitness value is achieved. Then the newest generation will be the final results. The optimal fitness can be defined as the output of fitness function reaches a pre-defined value (tolerance error), or the generation after pre-defined iterations.

6. EVALUATION OF THE RETRIEVAL ALGORITHM

6.1. Retrieval procedure

In section 5.1, the retrieval problem is formulated as an optimization problem of finding the minimal difference of the observed spectrum and model spectrum defined by the 8 unknowns. In order to increase the convergent rate in the retrieval, the intervals for the following 6 parameters are selected.

$$0\% \leq F_w \leq 100\% \tag{22}$$
$$0 \leq D_0 \leq 5 \tag{23}$$
$$-4 \leq \mu \leq 4 \tag{24}$$
$$0 \leq N_w^h \leq 80 \tag{25}$$
$$0 \leq \Lambda \leq 5 \tag{26}$$
$$0 \leq \sigma_b \leq 5 \tag{27}$$

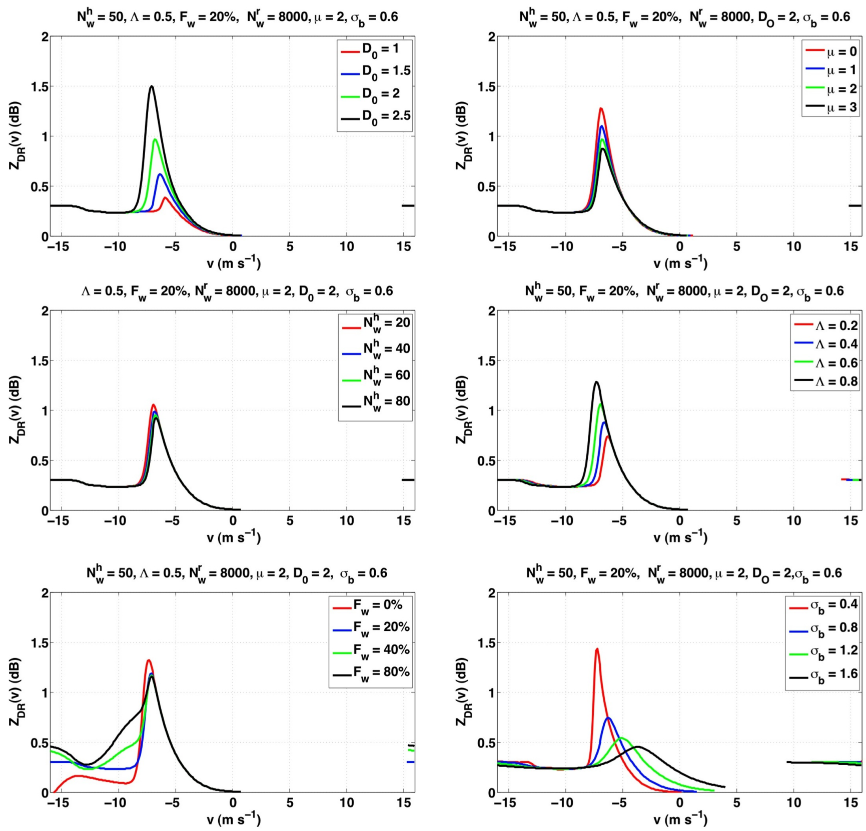

Figure 4: Similar to Fig. 3 but for $Z_{DR}(v)$.

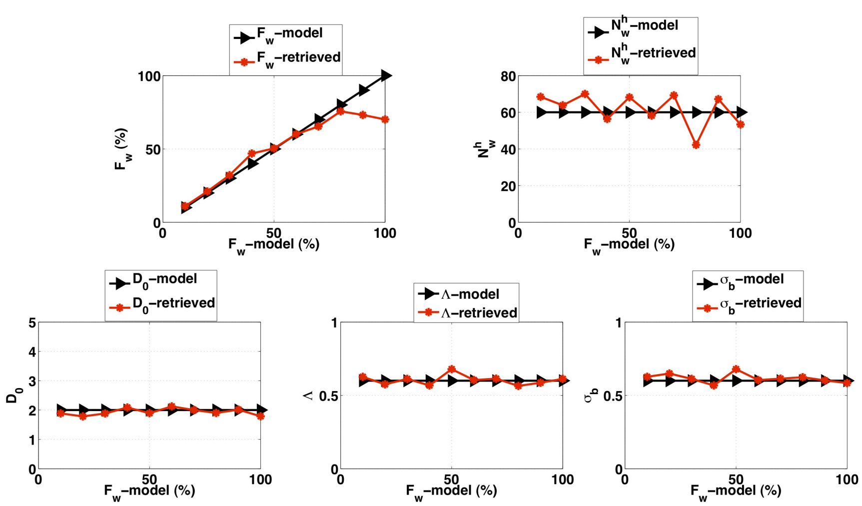

Figure 5: The retrieval results from F_w (top left), N_w^h (top right), D_0 (bottom left), Λ (bottom middle) and σ_b (bottom right) for different input F_w.

It should be noted that generally the interval of these parameters are not necessary for GA problems. However, in this work, some parameters have limited values from previous observations and research. For example, the melting ratio F_w should be between 0% and 100%. Therefore, optimal results can be reached with fewer iterations if the interval of these parameters are used. Following the procedure developed by Moisseev et al. [2006], one simplification was made by removing the estimation of the ambient air velocity v_0 from the GA fitting.

It should be noted that v_0 is estimated by finding the lag at which the cross correlation of modeled and measured spectra is maximum [Moisseev et al., 2006]. Moreover, in this work, in order to further decrease the statistical fluctuation, 20 Doppler spectra from two adjacent azimuth angles and 10 consecutive range gates are averaged.

The performance of the GA retrieval algorithm is demonstrated and evaluated in this section using simulations. The normalized error from initial guess and error after the retrieval is completed, is defined by $\epsilon_i = |\psi_m - \psi_i|/\psi_m$ and $\epsilon_r = |\psi_m - \psi_r|/\psi_m$, respectively, where ψ_m, ψ_i and ψ_r represent the model parameters, initial guess, and the retrieval results. The DSD parameters and the melting ratio of the model, initial guess, the mean and standard deviation of 30 realizations, and the mean ϵ_r ($\bar{\epsilon_r}$) are provided in Table 1. Since N_w^r has relative small effect on Doppler spectrum and has no effect on Z_{DR} spectrum as shown in section 4, large errors are expected in the retrieval result. The N_w^r in the model and initial guess is 8000 and 7000, respectively. The resultant mean and the standard deviation of the retrieval is 6947 and 1094, respectively. The high SD indicates the retrieval of N_w^r is unstable and sensitive to small changes in the Doppler spectrum. Similar to N_w^r, relative small effect on both spectra can explain the large SD of the retrieved μ, Better retrieval results can be observed for D_0, N_w^h, Λ, F_w and σ_b, which are manifested by small ϵ_r and small standard deviation. It is because these 5 parameters have significant effects on the Doppler spectrum and Z_{DR} spectrum compared to N_w^r and μ as shown previously.

The performance of the proposed retrieval technique is further tested and the impact of F_w on the retrieval is presented in Fig. 5. Large errors are likely to be generated in the retrieval of N_w^r and μ, and therefore they are not included in the sensitivity test. In Fig. 5, the $\mathrm{F_w}$-model is changed from 10% to 100% with step of 10%. The N_w^h, D_0, Λ and σ_b are set as 60, 2, 0.6 and 0.6, respectively. When $\mathrm{F_w}$-model change from 0% to 70%, the F_w can be retrieved accurately. However, after $\mathrm{F_w}$-model reaches 70%, the retrieved F_w exhibits large errors and fluctuates around approximately 70%. It can be explained by examining Figs. **??** and **??**, where $\mathrm{F_w}$-model has limited effect on Doppler spectrum and Z_{DR} spectrum after $\mathrm{F_w}$-model reaches 70%. Retrieval error of N_w^h can be observed with maximum ϵ_r of 0.2956 (when $F_w = 80\%$) and mean ϵ_r of 0.1279. On the other hand, it can be shown from from Fig. 5 that D_0, Λ and σ_b can be accurately retrieved with the mean ϵ_r of 0.0546, 0.0422 and 0.0431, respectively.

In the simulation, the elevation angle was 45^o, and 256 samples were used to generate the Doppler and Z_{DR} spectra. Moreover, 20 spectra were averaged in the retrieval to reduce the statistical fluctuations. In summary, the simulation results indicate that the GA algorithm can retrieve DSD parameters and melting ratio with small normalized errors and standard deviations.

7. CONCLUSION AND FUTURE WORK

In this work, a new technique to retrieve the DSDs of raindrops and melting hailstones as well as the melting ratio of hailstones was developed using Doppler and Z_{DR} spectra. As a part of the proposed method, the relationship between the melting ratio and the backscattering cross section of hailstones was obtained using polynomial fitting to the pre-calculated T-matrix results at C-band. It has been shown that the GA can provide reasonable retrieval in the optimization problem of multiple unknown parameters.

A microphysical model was developed for the mixture of raindrops and melting hailstones. This model depends on eight parameters: the gamma drop size distribution of raindrops (N_w^r, D_0 and μ) and hailstones (N_w^h and Λ), the melting ratio of hailstones (F_w), the spectral broadening (σ_b), and the ambient wind velocity (v_0). The output of the model is the Doppler spectrum and differential reflectivity spectrum. Moreover, it was suggested that the ambient wind velocity can be estimated independently through cross-correlation analysis. As a result, the retrieval becomes a minimization with 7 unknowns. Since the problem is designed to retrieve two types of hydrometeors (raindrops and melting hailstones), the presence of other type particles such as snow (mixture of air, water and ice) may produce additional errors in the retrieval.

Some assumptions and simplifications were made in the microphysical model of the hailstones. First, the shedding process was not considered although the shedding will change the DSD of raindrops. This algorithm retrieves the instant DSD of raindrops and hailstones

	Model Value	Initial Value	Retrieval Result	$\bar{\epsilon_r}$
N_w^r	8000	7000	6947 (mean) 1094 (std)	13.16$\%$
D_0	2	4.5	1.92 (mean) 0.077 (std)	4$\%$
μ	2	1	1.03 (mean) 0.3 (std)	48.5$\%$
N_w^h	60	40	63.51 (mean) 7.66 (std)	5.85$\%$
Λ	0.6	0.4	0.6125 (mean) 0.0832 (std)	2.08$\%$
F_w	60$\%$	10$\%$	61.376$\%$ (mean) 7.98$\%$ (std)	2.29$\%$
σ_b	0.6	0.2	0.6124 (mean) 0.012$\%$ (std)	2.07$\%$

Table 1: The DSD parameters and melting ratio of model, initial guess, and the mean and standard deviation of the retrieval results from 30 realizations.

only at relatively high elevation angles when the Doppler sorting is sufficient. Second, when a hailstone start to melt, the water fraction on the surface of the hailstone will decrease its terminal velocity. The amount of decrease in velocity is proportional to the amount of water on the hail's surface. Although few models were developed to describe relations between the melting and the terminal velocity of hailstones in previous work [e.g. Rasmussen et al., 1984b; Rasmussen and Heymsfield, 1987; List et al., 1973], however there is no well accepted model in current stage. Since the focus of this work is not the study of the terminal velocity under different melting ratios, the equation proposed by Mitchell [1996] was used in this work. The parameters in the model were obtained from the fitting results from plentiful hailstones samples from summer seasons, which could be used to represent the mean velocities under various melting ratios for each size. However, bias is expected in the terminal velocity calculation. Third, in order to mitigate the impact of random fluctuation on the retrieval results, spectra used for the retrieval have been averaged over 20 adjacent gates. In other words, the spatial resolution of the retrieval is compromised.

Since DSD and melting ratio retrieval is the most critical part of this study, it would be advantageous of validate the retrieved results. The special setup required by this retrieval (45^o elevation angle and higher) make it difficult to compare the retrieved parameters to in-situ instruments. However, indirect validations of the retrieved melting ratio, nonetheless, is still possible. Since the hailstones are assumed melting when they are falling, larger melting ratio is expected at low altitude compared to high altitude. Therefore retrieval algorithm can be tested at two different elevation angles (30^o and 45^o), and the melting ratio retrieved from 30^o is expected higher than from 45^o. Even this approach can not evaluate the performance quantitatively, but still can qualitatively show the feasibility of this algorithm in the melting ratio retrieval.

The spectral broadening has relative large influence on the retrieval accuracy. This is a general limitation applicable to most DSD parameters retrieval methods based on the analysis of spectra. The statistical analysis of the performance of this retrieval algorithm under different spectral broadening, elevation angle, FFT length, etc. is needed to further demonstrate the feasibility of the algorithm. Similar analysis can be found in the work from Moisseev et al. [2006]. Since unusual setting is required for the radar to collect the data for this research (elevation angle of 45^o and higher), and the mixture of raindrops and hailstones is not a very common type of precipitation, there is no real data collected for this work in current stage. Real case analysis is the most important part to validate the application of the proposed method, and will be implemented in future work.

8. ACKNOWLEDGMENT

This work was supported by the Enterprise Electronics Corporation (EEC) and WSI Corporation under the project of advanced tornado detection. The authors would also like to thanks the NSSL staff for the collection of Level I data.

References

Atlas, D., R. C. Srivastava, and R. S. Sekhon, 1973: Doppler radar characteristics of precipitation at vertical incidence. *Rev. Geophys. Space Phys.*, **11**, 1–35.

Balakrishnan, N., and D. S. Zrnić, 1990: Estimation of rain and hail rates in mixed-phase precipitation. *J. Atmos. Sci.*, **47**, 565–583.

Battan, L. J., and J. B. Theiss, 1973: Wind gradients and variance of Doppler spectra in showers viewed horizontally. *J. Appl. Meteorol.*, **12**, 688–693.

Bringi, V. N., and V. Chandrasekar, 2001: *Polarimetric Doppler Weather Radar Principles and Applications*. Cambridge University Press, Cambridge, UK.

Cheng, L., and M. English, 1983: A relationship between hailstone concentration and size. *J. Atmos. Sci.*, **40**, 204–213.

Doviak, R. J., and D. S. Zrnić, 1993: *Doppler Radar and Weather Observations*. Academic Press, San Diego, Calif., 130 pp.

Goddard, J. W. F., S. M. Cherry, and V. N. Bringi, 1982: Comparison of dual-polarized radar measurements of rain with ground-based disdrometer measurements. *J. Appl. Meteorol.*, **21**, 252–256.

Green, A. V., 1975: An approximation for shape of large raindrops. *J. Appl. Meteorol.*, **14**, 1578–1583.

Hendry, A., and G. C. McCormick, 1976: Radar observations of the alignment of precipitation particles by electrostatic fields in thunderstorms. *J. Geophys. Res.*, **81**, 5353–5357.

Jung, Y., G. Zhang, and M. Xue, 2007: Assimilation of simulated polarimetric radar data for a vonvective storm using the ensemble kalman filter. Part I: observation operators for reflectivity and polarimetric variables. *Mon. Weather Rev.*, **136**, 2228–2245.

Knight, N. C., 1982: Hailstone shape factor and its relation to radar interpretation of hail. *J. Climate Appl. Meteor.*, **25**, 1956–1958.

Law, J. O., and D. A. Parson, 1943: The relationship of raindrop size to intensity. *Trans. Amer. Geophys. Union.*, **24**, 452–460.

List, R., U. W. Rentsch, A. C. Byram, and E. P. Lozowski, 1973: On the aerodynamics of spheroidal hailstone models. *J. Appl. Meteorol.*, **30**, 653–661.

Marshall, J. S., and W. Palmer, 1948: The distribution of raindrops with size. *J. Meteor.*, **5**, 165–166.

Matson, R., and A. W. Huggins, 1980: The direct measurement of the sizes, shapes and kinematics of falling hailstones. *J. Atmos. Sci.*, **37**, 1107–1125.

Maxwell-Garnett, J. C., 1904: Colors in metal glasses and in metallic films. *Philos. Trans. Roy. Soc. London*, **A203**, 385–420.

Mitchell, D. L., 1996: Use of mass- and area-dimensional relationships for determining precipitation particle terminal velocities. *J. Appl. Meteorol.*, **53**, 1710–1723.

Moisseev, D. N., V. Chandrasekar, C. M. H. Unal, and H. W. J. Russchenberg, 2006: Dual-polarization spectral analysis for retrieval of effective raindrop shapes. *J. Atmos. Oceanic Technol.*, **23**, 1682–1695.

Nespor, V., W. F. Krajewski, and A. Kruger, 2000: Wind-induced error of rain drop size distribution measurement using a two-dimensional video disdrometer. *J. Atmos. Oceanic Technol.*, **17**, 1483–1492.

Pruppacher, H. R., and R. L. Pitter, 1971: A semi-empirical determination of the shape of cloud and rain drops. *J. Atmos. Sci.*, **28**, 86–94.

Rasmussen, R. M., and A. J. Heymsfield, 1987: Melting and shedding of graupel and hail. Part I: model physics. *J. Atmos. Sci.*, **19**, 2754–2763.

Rasmussen, R. M., V. Levizzani, and H. R. Pruppacher, 1984a: A wind tunnel and theoretical study on the melting behavior of atmospheric ice particles: III. experiment and theory for spherical ice particles of radius $<$ 500 um. *J. Atmos. Sci.*, **41**, 381–388.

Rasmussen, R. M., V. Levizzani, and H. R. Pruppacher, 1984b: A wind tunnel and theoretical study on the melting behavior of atmospheric ice particles: III. experiment and theory for spherical ice particles of radius $>$ 500 um. *J. Atmos. Sci.*, **41**, 381–388.

Sato, T., H. Doji, H. Iwai, I. Kimura, S. Fukao, M. Yamamoto, T. Tsuda, and S. Akto, 1990: Computer processing for deriving drop-size distributions and vertical air velocities from VHF Doppler radar spectra. *Radio Sci.*, **25**, 961–973.

Sellami, A., M. Zagrouba, M. Bouaicha, and B. Bessais, 2007: Application of genetic algorithms for the extraction of electrical parameters of multicrystalline silicon. *Meas. Sci. Technol*, **18**, 1472–1476.

Spek, A. L. J., C. M. H. Unal, D. N. Moisseev, H. W. J. Russchenberg, V. Chandrasekar, and Y. Dufournet, 2007: A new technique to categorize and retrieve the microphysical properties of ice particles above the melting layer using radar dual-polarization spectral analysis. *J. Atmos. Oceanic Technol.*, **25**, 482–497.

Ulbrich, C. W., 1983: Natural variations in the analytical form of the raindrop size distribution. *J. Climate Appl. Meteor.*, **22**, 1764–1775.

Wong, R., and N. Chidambaram, 1985: Gamma size distribution and stochastic sampling errors. *J. Appl. Meteorol.*, **24**, 568–579.

Zhang, G., J. Viekanandan, and E. Brandes, 2001: A method for estimating rain rate and drop size distribution from polarimetric radar measurements. *IEEE Trans. Geosci. Remote Sens.*, **39**, 830–841.